

Title	Enhanced performance of organic light-emitting diodes by inserting wide-energy-gap interlayer between hole-transport layer and light-emitting layer
Author(s)	Honda, Yusuke; Matsushima, Toshinori; Murata, Hideyuki
Citation	Thin Solid Films, 518(2): 545-547
Issue Date	2009-07-09
Type	Journal Article
Text version	author
URL	http://hdl.handle.net/10119/9198
Rights	NOTICE: This is the author's version of a work accepted for publication by Elsevier. Yusuke Honda, Toshinori Matsushima, Hideyuki Murata, Thin Solid Films, 518(2), 2009, 545-547, http://dx.doi.org/10.1016/j.tsf.2009.07.016
Description	



Enhanced performance of organic light-emitting diodes by inserting wide-energy-gap interlayer between hole-transport layer and light-emitting layer

Yusuke Honda, Toshinori Matsushima, Hideyuki Murata*

School of Materials Science, Japan Advanced Institute of Science and Technology,

1-1 Asahidai, Nomi, Ishikawa 923-1292, Japan

*Corresponding author. Tel.: +81 761 51 1531; Fax: +81 761 51 1149

E-mail address: murata-h@jaist.ac.jp

Abstract

We demonstrated that driving voltages, external quantum efficiencies, and power conversion efficiencies of organic light-emitting diodes (OLEDs) are improved by inserting a wide-energy-gap interlayer of (4,4'-*N,N'*-dicarbazole)biphenyl (CBP) between a hole-transport layer of *N,N*-di(naphthalen-1-yl)-*N,N'*-diphenyl-benzidine (α -NPD) and a light-emitting layer of tris(8-hydroxyquinoline)aluminum. By optimization of CBP thicknesses, the device with a 3-nm-thick CBP layer had the lowest driving voltage and the highest power conversion efficiency among the OLEDs. We attributed these improvements to enhancement of a carrier recombination efficiency and suppression of exciton-polaron annihilation. Moreover, we found that the degradation of the OLEDs is caused by decomposition of CBP molecules and excited-state α -NPD molecules.

Keywords: organic light-emitting diode, singlet-polaron annihilation, carrier recombination efficiency, degradation, unstable α -NPD excitons

1. Introduction

Recently, organic light-emitting diodes (OLEDs) have attracted much attention due to their high potentials for use in low-cost, large-area, flexible display, and lighting applications [1]. However, driving voltages, power conversion efficiencies, and operational stability of the OLEDs are still underdeveloped and must be improved for the practical applications. In general, organic fluorescent and phosphorescent molecules possess very long exciton lifetimes ranging typically from ns to μs [2] when compared with inorganic semiconductor materials. Due to the long exciton lifetimes, molecular excitons are quenched through various processes, such as exciton-exciton annihilation [3], exciton-polaron annihilation [4], and field-induced exciton dissociation [5], which result in a reduction in external quantum efficiency of the OLEDs in a high current density region [6]. In particular, Aziz *et al.* reported that excitons are strongly quenched by charge carriers built up at organic/organic heterojunction interfaces [7]. If this exciton quenching process at the interfaces can be suppressed, a marked improvement of the OLED performance will be possible.

In a standard bilayer OLED using *N,N*-di(naphthalen-1-yl)-*N,N'*-diphenyl-benzidine (α -NPD) as a hole-transport layer (HTL) and tris(8-hydroxyquinoline)aluminum (Alq_3) as an emitting electron-transport layer (ETL), it is widely known that a large number of holes is built up at the interface of α -NPD and Alq_3 [8]. The built-up holes are expected to induce strong quenching of Alq_3 excitons generated near the interface. In this study, we used a wide-energy-gap interlayer (ITL) of (4,4'-*N,N'*-dicarbazole)biphenyl (CBP) between the α -NPD and the Alq_3 to prevent the

exciton quenching. Since a highest occupied molecular orbital (HOMO) energy level of CBP (-6.3 eV) is much deeper than that of α -NPD (-5.4 eV), holes are built up at the α -NPD/CBP interface separated away from the excitation generation region in the Alq₃ layer, suppressing the exciton quenching. By optimization of CBP thicknesses, we found that the device with a 3-nm-thick CBP layer had the highest power conversion efficiency together with the lowest driving voltage among the OLEDs. Moreover, degradation mechanisms of the OLEDs have not yet been understood and must be completely clarified for development of OLEDs. Thus, we discussed the degradation mechanisms of the OLEDs in the latter part of this report. We found that the degradation of our OLEDs is caused by decomposition of unstable CBP molecules and unstable excited-state α -NPD molecules.

2. Experimental

The OLED structures used in this study, the devices (A) and (B), are shown in Figs. 1(a) and 1(b), respectively. The devices (A) were composed of a glass substrate coated with a 150 nm anode layer of indium tin oxide (ITO) with a sheet resistance of 10 Ω /sq, a 0.75 nm hole-injection layer of MoO₃ [9], a 50 nm α -NPD HTL, an X nm CBP ITL, a 65 nm Alq₃ light-emitting ETL, a 0.5 nm LiF electron-injection layer, and a 100 nm Al cathode layer. In the devices (A), the CBP thickness X was changed from 0 nm to 10 nm. To investigate the degradation mechanisms, we also fabricated the device (B), where a 10 nm CBP ITL and a mixed layer of α -NPD and Alq₃ (1:1 by mol) were embedded.

Glass substrates coated with an ITO layer were cleaned using ultrasonication in acetone, followed by ultrasonication in detergent, pure water, and isopropanol. Then, the substrates were

treated by UV ozone for 30 min. All inorganic and organic layers were successively vacuum-deposited on the cleaned ITO layer, under a base pressure of 10^{-6} Pa, to fabricate the device structures shown in Figs. 1(a) and 1(b). The active area of the devices was defined at 4 mm^2 by the overlapped area of the ITO and the Al. The deposition rates were 0.01 nm/s for the MoO_3 layer, 0.1 nm/s for the organic layers, 0.05 nm/s for the LiF layer, and 0.3 nm/s for the Al layer. After the Al deposition, the devices were immediately encapsulated with a glass cap in a dry nitrogen-filled glove box. The current density-voltage-external quantum efficiency (J - V - η_{ext}) characteristics of the devices were measured with a Keithley 4200 semiconductor parameter analyzer system and an integrating sphere equipped with a Si photodiode (S2281, Hamamatsu photonics). The power conversion efficiencies (η_{power}) of the devices were measured using a luminance meter (BM-9, Topcon). The electroluminescence (EL) spectra of the devices were measured at a current density of 50 mA/cm^2 using a Keithley 2400 source meter and an Ocean Optics USB-2000 fiber optic spectrometer. To evaluate the operational stability, the devices were continuously operated at a current density of 50 mA/cm^2 . All measurements were conducted at room temperature.

3. Results and discussion

Figure 2 shows the J - η_{ext} characteristics of the devices (A) with various X . The η_{ext} was improved by inserting the CBP ITL between the α -NPD and the Alq_3 . We suppose that the enhanced η_{ext} is mainly attributable to the suppression of Alq_3 excitation quenching caused by the holes built up at the heterojunction interface. Since a hole mobility of α -NPD ($(3.0\text{-}10.0) \times 10^{-4} \text{ cm}^2/\text{V s}$) [10,11] is much higher than an electron mobility of Alq_3 ($(3.0\text{-}9.0) \times 10^{-5} \text{ cm}^2/\text{V s}$) [12], the large difference in the mobilities induces an imbalance in the number of injected holes and

electrons in the Alq₃ layer. Thus, the improvement of a carrier balance factor by using the CBP ITL is expected to enhance the η_{ext} as well.

The J - V characteristics of the devices (A) are shown in the inset in Fig. 3. The V decreased by inserting the 3-nm-thick CBP ITL between the α -NPD and the Alq₃, which is attributable to the improvement of a carrier recombination efficiency in the Alq₃ layer [13,14]. Reversely, the V increased when increasing the X from 3 to 10 nm. This voltage increase may be due to an increase in total film thickness.

The η_{power} - X characteristics of the devices (A) operated at a current density of 50 mA/cm² were shown in Fig. 3. The device with an X of 3 nm had the highest η_{power} among the devices due to the increase in the η_{ext} and the reduction in the V as discussed above. From these, we concluded that the optimized X is 3 nm, which provided the lowest V and the highest η_{power} for the device.

Figure 4 shows the luminance/initial luminance-time and driving voltage-time characteristics of the devices (A) operated at a current density of 50 mA/cm². By contrast with the improvements of the η_{ext} , the V , and the η_{power} , the operational lifetimes were degraded as the X was increased from 0 nm to 10 nm. Kondakov *et al* reported that CBP is electrochemically decomposed during device operation [15]. Since electrochemically decomposed species act as nonradiative recombination centers and/or luminance quenchers in a carrier recombination zone, EL efficiencies of OLEDs gradually decrease as the amount of decomposed species increases with operational time [16]. Based on this discussion, we assume that the degradation of the

OLEDs is mainly caused by the electrochemical decomposition of CBP molecules. In addition to this mechanism, we should point out that excited-state α -NPD molecules are unstable and the generation of electrochemically decomposed α -NPD species also accelerate the OLED degradation. The observation of the EL peaks originating from α -NPD at a shorter wavelength (≈ 430 nm) is the evidence that excitons and holes are recombined in the α -NPD layer to generate electrically excited α -NPD molecules (see the inset of Fig. 4).

To verify this hypothesis, we fabricated the device (B) where a 5 nm α -NPD:Alq₃ mixed layer was embedded in the α -NPD layer. Using this device structure, an energy transfer from excited-state α -NPD to ground-state Alq₃ is expected to occur to reduce the number of excited-state α -NPD molecules. The luminance/initial luminance-time and driving voltage-time characteristics of the device (A) with $X = 10$ nm and the device (B) are compared in Fig. 5. The EL spectra of these devices are shown in the inset of Fig. 5. From the lifetime characteristics and the EL spectra, we found that the OLED stability is enhanced when the α -NPD EL peak disappeared. This suggests that decomposition of excited-state α -NPD molecules would be one of the degradation mechanisms of the OLEDs.

4. Summary

We demonstrated that V , η_{ext} , and η_{power} of OLEDs are improved by inserting a CBP ITL between an α -NPD HTL and an Alq₃ ETL. We attributed these improvements to enhancement of a carrier recombination efficiency and suppression of exciton-polaron annihilation. We proposed that the degradation of the OLEDs is caused by unstable excited-state α -NPD molecules. By

replacing the CBP with a more electrochemically stable material, our technique using the wide-energy-gap ITL will be useful for overall enhancement of OLED performance.

References

- [1] C. W. Tang, S. A. VanSlyke, *Appl. Phys. Lett.* 51 (1987) 913.
- [2] M. A. Baldo, S. R. Forrest, *Phys. Rev. B* 62 (2000) 10958.
- [3] M. A. Baldo, C. Adachi, S. R. Forrest, *Phys. Rev. B* 62 (2000) 10967.
- [4] C. Adachi, M. A. Baldo, M. E. Thompson, S. R. Forrest, *J. Appl. Phys.* 90 (2001) 5048.
- [5] J. Kalinowski, W. Stampor, J. Mezyk, M. Cocchi, D. Virgili, V. Fattori, P. Di. Marco, *Phys. Rev. B* 66 (2002) 235321.
- [6] M. A. Baldo, S. Lamansky, P. E. Burrows, M. E. Thompson, S. R. Forrest, *Appl. Phys. Lett.* 86 (2005) 213506.
- [7] Y. Luo, H. Aziz, G. Xu, Z. D. Popovic, *Chem. Mater.* 19 (2007) 2288.
- [8] Y. Noguchi, N. Sato, Y. Tanaka, Y. Nakayama, H. Ishii, *Appl. Phys. Lett.* 92 (2008) 203306.
- [9] T. Matsushima, G.-H. Jin, H. Murata, *J. Appl. Phys.* 104 (2008) 054501.
- [10] Z. Deng, S. T. Lee, D. P. Webb, Y. C. Chan, W. A. Gambling, *Synth. Met.* 107 (1999) 107.
- [11] S. Naka, H. Okada, H. Onnagawa, Y. Yamaguchi, T. Tsutsui, *Synth. Met.* 111 (2000) 331.
- [12] R. A. Klenkler, G. Xu, H. Aziz, Z. D. Popovic, *Appl. Phys. Lett.* 88 (2006) 242101.
- [13] J. Kalinowski, L. C. Palilis, W. H. Kim, Z. H. Kafafi, *J. Appl. Phys.* 92 (1998) 12.
- [14] J. Kalinowski, L. C. Picciolo, H. Murata, Z. H. Kafafi, *J. Appl. Phys.* 89 (2001) 1866.
- [15] D. Y. Kondakov, W. C. Lenhart, W. F. Nichols, *J. Appl. Phys.* 101 (2007) 024512.
- [16] D. Y. Kondakov, J. R. Sandifer, C. W. Tang, R. H. Young, *J. Appl. Phys.* 93 (2003) 15.

Figure captions

Fig. 1. Schematic structures of devices (A) and device (B). In devices (A), CBP thickness X was changed from 0 nm to 10 nm. In device (B), 10 nm CBP layer and 5 nm mixed layer of α -NPD and Alq₃ (1:1 by mol) were used.

Fig. 2. External quantum efficiency-current density ($\eta_{\text{ext}}-J$) characteristics of devices (A) with various X . Inset shows current density-voltage ($J-V$) characteristics of devices (A) with various X .

Fig. 3. Power conversion efficiency-CBP thickness ($\eta_{\text{power}}-X$) characteristics of devices (A) operated at current density of 50 mA/cm².

Fig. 4. Luminance/initial luminance-time and driving voltage-time characteristics of devices (A) with various X . Devices were operated at current density of 50 mA/cm². Inset shows EL spectra of devices (A) at current density of 50 mA/cm². EL peaks at ≈ 430 nm and ≈ 520 nm in inset originate from α -NPD and Alq₃, respectively.

Fig. 5. Luminance/initial luminance-time and driving voltage-time characteristics of device (A) with $X = 10$ nm and device (B). These devices were operated at current density of 50 mA/cm². Inset shows EL spectra of device (A) with $X = 10$ nm and device (B) at current density of 50 mA/cm².

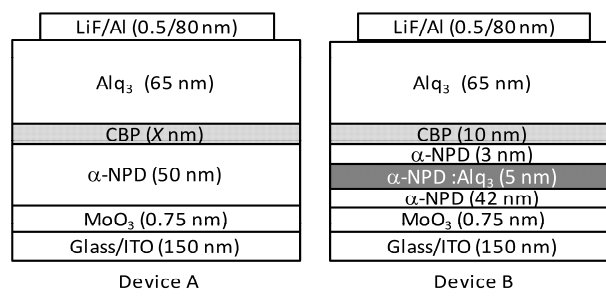


Fig. 1.

Honda *et al.*

Thin Solid Films

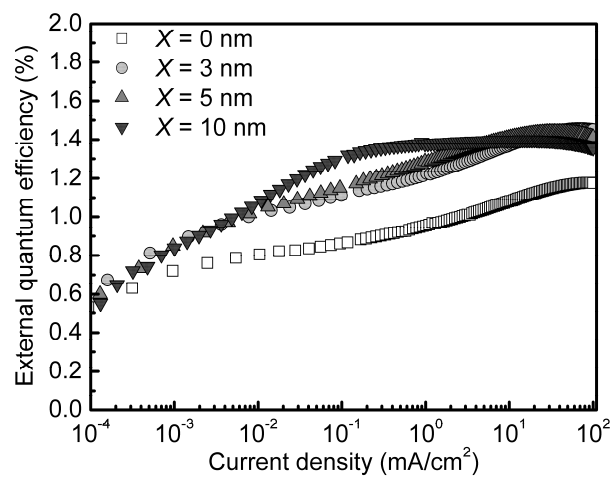


Fig. 2.

Honda *et al.*

Thin Solid Films

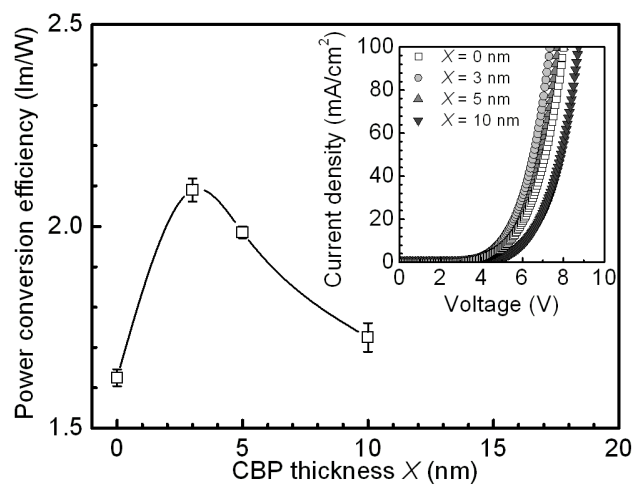


Fig. 3.

Honda *et al.*

Thin Solid Films

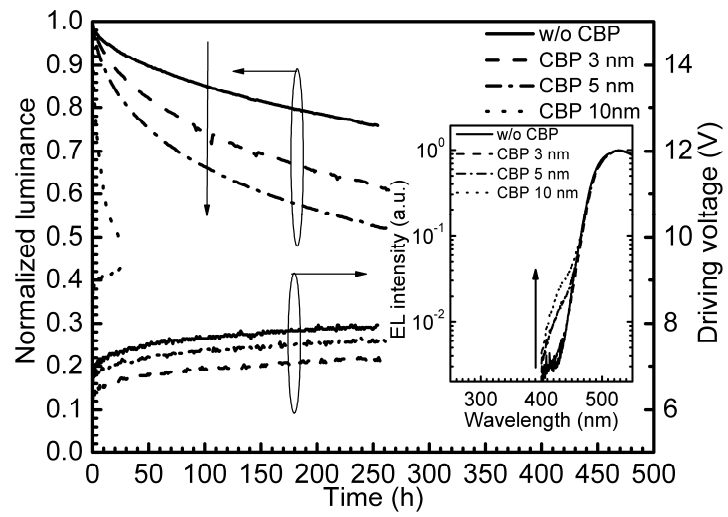


Fig. 4.

Honda *et al.*

Thin Solid Films

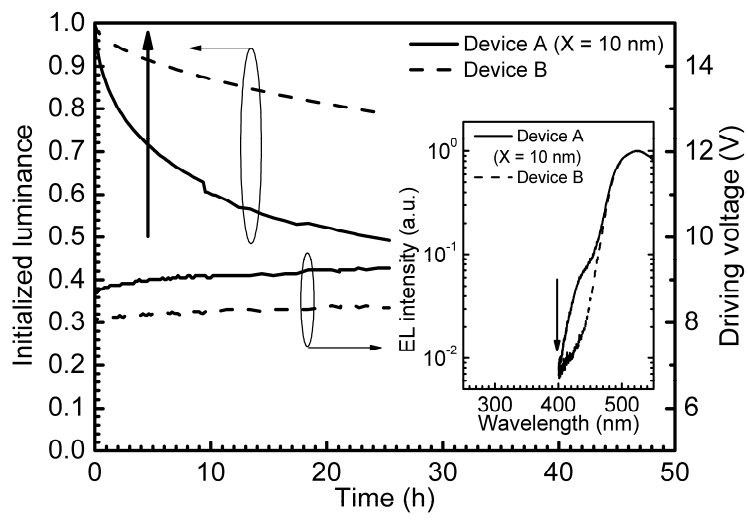


Fig. 5.

Honda *et al.*

Thin Solid Films